ChemComm

Accepted Manuscript

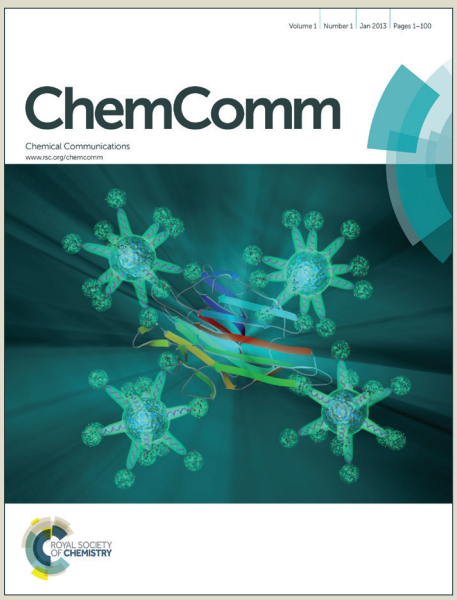

ROYAL SOCIETY OF CHEMISTRY

www.rsc.org/chemcomm

Cite this: DOI: 10.1039/c0xx00000x

www.rsc.org/xxxxxx

ARTICLE TYPE

In situ preparation of 3D graphene aerogels@hierarchical Fe_3O_4 nanoclustersas high rate and long cycle anode materials for lithium ion batteries

Lishuang Fan,[c] Bingjiang Li,[c] David W. Rooney,[d] Naiqing Zhang*[a,b] and Kening Sun*[ab]

Received (in XXX, XXX) XthXXXXXXXXX 20XX, Accepted Xth XXXXXXXXX 20XX
DOI: 10.1039/b000000x

We describe a novel strategy for in situ fabrication of hierarchical Fe_3O_4 nanoclusters/GAs. Fe_3O_4 NCs/GAs deliver an excellent rate capability (the reversible capacities obtained were 1442, 392 and 118 $mAhg^{-1}$ at 0.1C, 12C and 35C rates), and a high reversible capacity of 577 mAh g^{-1}over 300 cycles at the current density of 5.2 A/g (6C).

Rechargeable lithium-ion batteries (LIB) are key device for mobile communication devices, portable electronic devices, and electrical/hybrid vehicles (EVs/EHVs). The main challenges in this field are achieving high capacity, excellent cycling performance and rate capability for both anode and cathode materials to meet the increasing power supply requirements for a variety of applications.[1] However, the limited theoretical capacity of 372 $mAhg^{-1}$ of the commercial anode material of graphite cannot fully meet the requirement.[2] For the purpose of improving the electrochemical performance of LIBs, considerable efforts have been made recently in searching new electrode materials, which always have higher energy density compared with the existing system.[3] Fe_3O_4 is considered as a promising anode material candidate because of its high theoretical capacity, natural abundance, nontoxic nature, and low cost.[3d, 4] Nevertheless, its application in practical LIB is hindered due to its low rate performance arising from kinetic limitations due to low intrinsic electric conductivity and poor cycling stability resulting from large volume expansion occurring during cycling.[5] For these challenges, some strategies have been made to resolve these issues significantly. The first strategy is to introduce Fe_3O_4 nanostructure resulting in shorter path lengths for the transport of electrons and lithium ions.[3b,6] The other promising strategy is to construct hybrid electrodes composed of Fe_3O_4 and conductive additive providing rapid electron channel.[3d,4a,4c,5a, 7]

More recently, compared with 2D graphene, 3D graphene aerogels (GAs) have drawn much more attention due to its strong mechanical strengths, fast mass and electron transport rate benefiting from the 3D interconnected framework and the intriguing properties of graphene. Therefore, constructing GAs hybrid 3D hierarchical Fe_3O_4 will be an effective way to achieve both longer cycling life and higher rate performance for LIBs.

In this work, we describe a novel strategy which is both facile and cost effective for in situ fabrication of 3D hierarchical Fe_3O_4 nanoclusters /GAs (Fe_3O_4 NCs/GAs). Herein, hierarchical Fe_3O_4 NCs can effectively bring down the mean diffusion time of the lithium ions by minimizing the diffusion length, and the GAs provide protection against the volume changes of Fe_3O_4 NCs in 3D space during electrochemical process. Meanwhile, the interconnected 3D networks and channel abundance can enhance the electrical conductivity and ion diffusion.

The fabrication process of 3D Fe_3O_4 NCs/GAs is illustrated in Figure 1a (the detail in ESI). The morphology and microstructure of Fe_3O_4 NCs and Fe_3O_4 NCs/GAs were examined by scanning electron microscopy (SEM), transmission electron microscope (TEM), and high resolution TEM (HRTEM) measurement. SEM and TEM images confirm that Fe_3O_4 NCs shown uniformly nanocluster structure (Figure S1) and the Fe_3O_4NCs are well wrapped by the graphene (Figure 1b, c). This feature can be characterized by EDX mapping of the elements C, Fe, and O. Remarkablely, Fe_3O_4 nanoclusters were assembled by tiny Fe_3O_4

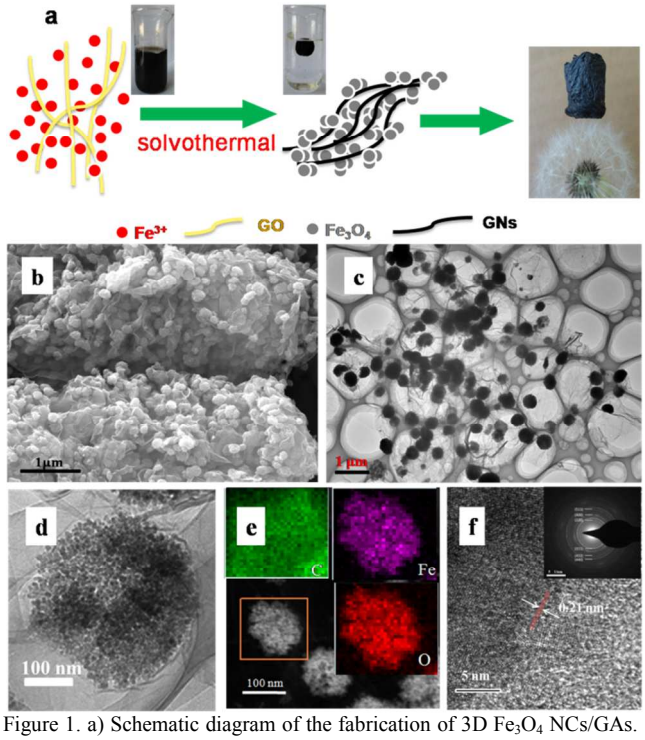

Figure 1. a) Schematic diagram of the fabrication of 3D Fe_3O_4 NCs/GAs. b, c, d) SEM and TEM image of the Fe_3O_4NCs/GAs. e, f) The

corresponding elemental mapping (C, Fe and O) and HRTEM images of Fe_3O_4 NCs/GAs, inset: SAED pattern.

nanoparticles (5nm) .The SAED pattern of a single Fe_3O_4 NCs shows a very light ring-pattern in Figure 1e. The diffraction rings can be indexed to (200), (311), (400), (422), (440) and (511) planes of a face-centered cubic magnetite phase.

The pattern confirmed the formation of Fe_3O_4 (JCPDS no.19-0629) in the Fe_3O_4 NCs/GAs (Figure 2a).[8] From the TGA, it was estimated that the amount of graphene in the composites was about ~33 wt% (Figure S2). Brunauer-Emmett-Teller analysis shows a specific surface area of 118 m^2/g for Fe_3O_4 NCs/GAs (Figure 2b), which is much higher than the previously reported for Fe_3O_4/graphene composites.[4c,9] The observed type hysteresis loop confirms the mesoporous structure. Based on the Barrett-Joyner-Halenda model, a well-defined mesopore (5.6nm) was obtained (Figure S3), which contributed to the pores existing between the Fe_3O_4 NPs. The mesoporous configuration benefits electrolyte diffusion to active sites. The macropores of 50-250 nm attribute to the pores existing between nanocluster and 3D graphene, which is benefit to transport of the electrolyte and enhancing the rate performance.[10] The Fe 2p XPS spectrum of the Fe_3O_4 NCs/GAs (Figure S4) exhibits two peaks at 710.7 and 724.8 eV, corresponding to the Fe $2p_{3/2}$ and Fe $2p_{1/2}$ of Fe_3O_4.[8a,9a,9b,11] The presence of Fe_3O_4 can be further confirmed by the O1s predominant peak at 533.0 eV, which corresponds to the oxygen species in the Fe_3O_4 phase.[11]

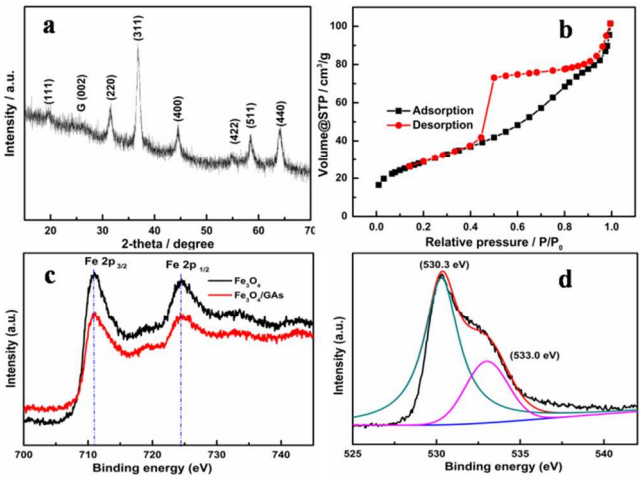

Figure 2. a) XRD profiles of Fe_3O_4 NCs/GAs composite. b) N_2 adsorption/desorption isotherms of Fe_3O_4 NCs/GAs. c,d) XPS spectrum of the Fe_3O_4 NCs/GAs and Fe_3O_4, and the high resolution spectra of Fe 2p and O 1s.

The insertion/extraction of Fe_3O_4 NCs/GAs anodes was characterized using cyclic voltammetry (CV). As shown in Figure 3a, three peaks, located at 1.58, 0.90 and 0.75 V, were observed in the first insertion process. The two insertion peaks at higher voltage disappeared in the subsequent cycles, and they were possibly attributed to lithium intercalation to formation $Li_xFe_3O_4$[12] and the formation of a solid electrolyte interphase (SEI) film caused by the decomposition of electrolyte, which contributes to the irreversible capacity, as well as the three steps of the lithiation reaction of Fe_3O_4.[8b,13] The sharp reduction peak at about 0.75 V is observed in the first cathodic scan for the Fe_3O_4 NCs/GAs, which can be attributed to the reduction of Fe^{3+}/Fe^{2+} to Fe^0. The extraction process presents two well-defined peaks at 1.61 and 1.81 V, which are attributed to the reversible

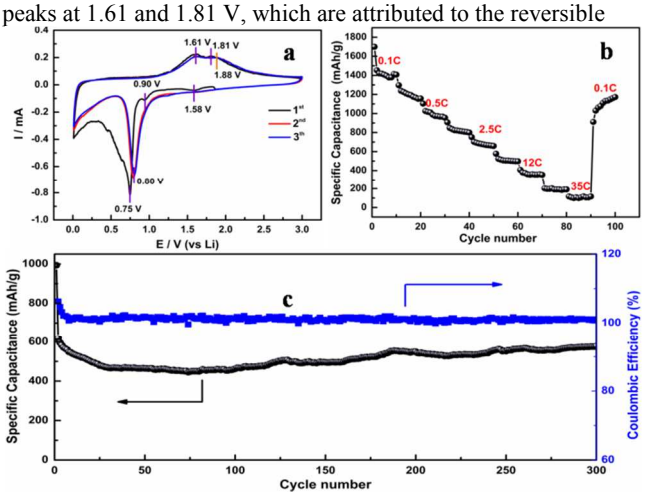

Figure3. a) CV curve of Fe_3O_4 NCs/GAs nanocomposites in the potential window 0.01V-3V with 0.01mV/s scanning rate. b) Rate performance of the Fe_3O_4 NCs/GAs nanocomposites at different current densities. c) Cycling performance of the Fe_3O_4 NCs/GAs nanocomposites at a current density of 6C for 300 cycles.

oxidation of Fe^0 to Fe^{2+}/Fe^{3+}.[13b,14] From the second cycle, both cathodic and anodic peaks are positively shifted in the subsequent cycles which attribute to the structural modification after the first cycle due to lithium insertion and extraction,[12a-b,13a] which is easy to insertion. It also worth noted that the peaks at 0.8 V during discharge and at 1.61 and 1.81 V during charge ($Fe_3O_4 \leftrightarrow$ Fe) for the second or third cycles of the Fe_3O_4 NCs/GAs electrode are almost overlapped. This can be indexed to the high reversibility of Fe_3O_4 NCs/GAs, indicating that the unique structure can improve the sufficient oxidation reaction process during the anodic cycling and insure excellent reversibility of the Fe_3O_4 NCs/GAs anode.

Galvanostatic discharge/charge at 0.1C of the cell exhibited a first cycle reversible capacity of 1442 $mAhg^{-1}$ (Figure S5).The reversible capacity observed is higher than the theoretical capacity for Fe_3O_4based anodes, which is 926 $mAhg^{-1}$ following an $8e^-$ transfer reaction per formula weight.[8a,9a-b,10,13c,14] However, such higher-than-theoretical capacity values have been observed before for transition metal oxides anodes, which is attributed to the formation of a pseudo-capacitive gel like film.[4d,13c,14] The reversible capacities obtained were 1442, 1221, 1020 and 845 $mAhg^{-1}$ for 0.1, 0.2, 0.5 and 1.2 C rates (considering 865 mAg^{-1} as 1C for simplicity Figure 3c, S6), respectively. The cell was further cycled at an extremely high current rate of 12 C and 35 C for 10 cycles. The reversible specific capacity was 392 and 118 $mAhg^{-1}$. Additionally, the capacity was exceptionally stable at such a high current rate. More importantly, when the current rate was set back to 0.1C after such high rate cycling, the capacity of the cell recovered to 1200 $mAhg^{-1}$, suggesting that the hierarchical nanostructure was not dramatically affected by the high rate charge/discharge cycles.

The cyclic stability of Fe_3O_4+GAs and Fe_3O_4 NCs/GAs was measured. The capacity and cyclic stability of the Fe_3O_4 NCs/GAs composite are higher than the Fe_3O_4+GAs at a 1C (Figure S7), which attribute to the strong anchoring of Fe_3O_4 NCs on GAs empowers fast electron transport through graphene layers

to Fe_3O_4 NCs to enhance the electrochemical performance. A cell was cycled at 5200 mAg^{-1} (i.e. 6C) for 300 cycles (Figure 3c). Fe_3O_4 NCs/GAs composite presents excellent cycling stability with the initial discharge capacity of 1000 mAh g^{-1} and the discharge capacity of 577 $mAhg^{-1}$ until 300 cycles. To our knowledge, the 3D hierarchical Fe_3O_4 NCs/GAs composite shows excellent C-rate retention and cycling capability than the anodes of Fe_3O_4 or Fe_3O_4 graphene hybrids/composition reported in recent literature,[4-7,8,9a-b, 13c,14] which good confinement of active materials by the graphene 3D network and Fe_3O_4 NCs further compensated for the volume due to ultrasmall nanoparticles of Fe_3O_4 NCs and the effective nanopores each other (Figure S8,9).

To verify the good performance of the Fe_3O_4 NCs/GAs, ac impedance measurements were also conducted as shown in Figure S10, which indicates that the charge-transfer resistances of the Fe_3O_4 NCs/GAs electrodes are smaller than Fe_3O_4 electrode. In addition, we also found that the diameter of the semicircle was decrease after 300 cycles for Fe_3O_4 NCs/GAs. Therefore, it can be assumed that the Fe_3O_4 inter-particle resistance of the electrode was suppressed by the *in situ* self-assembly GAs. This result demonstrated that the GAs serves as a conductive network, which improves the local conductivity, and then leads to a high electrochemical performance for the Fe_3O_4 NCs/GAs electrodes as anode materials for LIBs.

Conclusions

In conclusion, novel hierarchical Fe_3O_4 NCs encapsulated in GAs (Fe_3O_4 NCs/GAs) have been successfully fabricated by a facile and scalable *in situ* synthesis method. In this architecture, hierarchical Fe_3O_4 NCs can suppress the stacking of graphene layers, and effectively bring down the mean diffusion time of the lithium ions. The GAs can effectively accommodate the mechanical stress induced by the volume change of embedded Fe_3O_4 and provide excellent electron transfer and ion diffusion during the charge and discharge processes. Due to the synergistic effects, the Fe_3O_4 NCs/GAs exhibits an extremely excellent rate capability (The reversible capacities obtained were 392 and 118 $mAhg^{-1}$ for 12 C and 35 C rates), and a long cycle performance (reversible capacity of 577 mAh g^{-1} over 300 cycles at the current density of 5.2 A/g).

This work was supported by State Key Laboratory of Urban Water Resource and Environment, Harbin Institute of Technology, No.2013TS08 and the Fundamental Research Funds for the Central Universities (Grant No.HIT.IBRSEM.A.201408).

Notes and references

[a]*State Key Laboratory of Urban Water Resource and Environment,* [b]*Academy of Fundamental and Interdisciplinary Sciences, Harbin Institute of Technology, Harbin, China. Fax: +86 451-86412153; Tel: XX +86 451-86412153; E-mail: znqmww@163.com*
[c]*Department of Chemistry, Harbin Institute of Technology.*
[d]*School of Chemistry and Chemical Engineering/QUILL Research Centre, Queen's University.*

† Electronic Supplementary Information (ESI) available: [details of experemental, CV and EIS]. See DOI: 10.1039/b000000x/

1 a) M.R. Palacin, *Chemical Society Reviews***2009**, 38, 2565. b) M. Armand, J.M. Tarascon, *Nature* **2008**, 451, 652. c) B. Dunn, H. Kamath, *Science* **2011**, 334, 928. d) J.M. Tarascon, M. Armand, *Nature* **2001**, 414, 359. e) J. B. Goodenough, Y. Kim, *Chem. Mater.* **2010**,22, 587.

2 a) A. Manthiram, *J. Phys. Chem. Lett.* **2011**, 2, 176. b) J. Cabana, L. Monconduit, D. Larcher, M.R. Palacin, *Adv.Mater.* **2010**, 22, E170.

3 a) Y. Idota, T. Kubota, A. Matsufuji, Y. Maekawa, T. Miyasaka, *Science* **1997**, 276, 1395. b) P. Poizot, S. Laruelle, S.Grugeon, L. Dupont, J.M. Tarascon, *Nature* **2000**, 407, 496. c) C.K. Chan, H. Peng, G. Liu, K.M. Wrath, X.F. Zhang, R.A. Huggins, Y. Cui, *Nat. Nanotechnol.* **2008**, 3, 31. d) P.L. Taberna, S. Mitra, P. Poizot, P. Simon, J.M. Tarascon, *Nat.Mater.* **2006**, 5, 567. e) S.M. Xu, C.M. Hessel, H. Ren, R.B. Yu, Q. Jin, M. Yang, H.J. Zhao, D. Wang, *Energy. Environ. Sci.* **2014**, 7, 632. f) J.Y. Wang, N.L. Yang, H.J. Tang, Z.H. Dong, Q. Jin, M. Yang, D. Kisailus, H.J. Zhao, Z.Y. Tang, D. Wang, *Angew. Chem. Int. Ed.* **2013**, 52, 6417. g) X.L. Jia, Z. Chen, X. Cui, Y.T. Peng, X.L. Wang, G. Wang, F. Wei, Y.F. Lu, *ACS Nano*, 2012, 6, 9911. h) X.J. Zhu, Y.W. Zhu, S. Murali, M.D. Stoller, R.S. Ruoff, ACS Nano, 2011, 5, 3333.

4 a) Z.S. Wu, W.C. Ren, L. Wen, L.B. Gao, J.P. Zhao, Z.P. Chen, G.M. Zhou, F. Li, H.M. Cheng, *ACS Nano* **2010**, 4, 3187. b) Z.M. Cui, L.Y. Hang,W.G. Song, Y.G. Guo, *Chem. Mater.* **2009**, 21, 1162. c) G.M. Zhou, D.W. Wang, F. Li, L.L. Zhang, N. Li, Z.S. Wu, L. Wen, G.Q. Lu, H.M. Cheng, *Chem. Mater.* **2010**, 22, 5306. d) Y. He, L. Huang, J.S. Cai, X.M. Zheng, S.G. Sun, *Electrochim.Acta* **2010**, 55, 1140.

5 a) T. Muraliganth, A.V. Murugan, A. Manthiram, *Chem. Commun.* **2009**, 47, 7360. b) N. Kang, J.H. Park, J. Choi, J. Jin, J. Chun, I.G. Jung, J. Jeong, J.G. Park, S.M. Lee, H.J. Kim, S.U. Son, *Angew. Chem. Int. Ed.* **2012**, 51, 6626. c) L.W. Ji, Z. Lin, M. Alcoutlabi, X.W. Zhang, *Energy. Environ. Sci.* **2011**, 4, 2682. d) J.S. Chen, Y.M. Zhang, (David) X.W. Lou, *ACS Appl. Mater. Interfaces* **2011**, 3, 3276.

6 a) J. Maier, *Nat. Mater.* **2005**, 4, 805, b) B. Koo, H. Xiong, M.D. Slater,V.B. Prakapenka, M. Balasubramanian, P. Podsiadlo, C.S. Johnson, T. Rajh, E.V. Shevchenko,*Nano Lett.* **2012**, 12, 2429. c) S. Wang, J. Zhang, C. Chen, *J. Power Sources* **2010**, 195, 5379. d) H. Duan, J. Gnanaraj, X. Chen, B. Li, J. Liang, *J. Power Sources* **2008**, 185, 512. e) F.S. Ke, L. Huang, B. Zhang, G.Z. Wei, L.J. Xue, J.T. Li, S.G. Sun, *Electrochim. Acta* **2012**, 78, 585. f) S.K. Behera, *J. Power Sources* **2011**, 196, 8669. g) M. Sasidharan, N. Gunawardhana, M. Yoshio, K. Nakashima, *Ionics***2013**, 19, 25. h) H.-S. Lim, B.-Y. Jung, Y.-K. Sun, K.-D. Suh, *Electrochem. Acta* **2012**, 75, 123. i) D.W. Su, H.-J. Ahn, G.X. Wang, *J. Power Sources* **2013**, 244, 742. j) 6J.S. Xu, Y.-J. Zhu, F. Chen, *J. Solid State Chemistry* **2013**, 199, 204.

7 a) W.M. Zhang, X.L. Wu, J.S. Hu, Y.G. Guo, L.J. Wan, *Adv. Funct. Mater.* **2008**, 18, 3941. b) C.M. Ban, Z.C. Wu, D.T. Gillaspie, L. Chen, Y.F. Yan, J.L. Blackburn, A.C. Dillon, *Adv. Mater.* **2010**, 22, E145. c) W.F. Chen, S.R. Li, C.H. Chen, L.F. Yan, *Adv. Mater.* **2011**, 23, 5679. d) E. Kang, Y.S. Jung, A.S. Cavanagh, G.H. Kim, S.M. George, A.C. Dillon, J.K. Kim, J. Lee, *Adv. Funct. Mater.* **2011**, 21, 2430. e) T. Zhu, J.S. Chen, (David) X.W. Lou, *J Phys. Chem. C* **2011**, 115, 9814.

8 a) W. Wei, S.B. Yang, H.X. Zhou, I. Lieberwirth, X.L. Feng, K. Müllen, *Adv. Mater.* **2013**, 25, 2909. b) W.-L. Chiang, C.-J. Ke, Z.-X. Liao, S.-Y. Chen, F.-R. Chen, C.-Y. Tsai, Y.N. Xia, H.-W. Sung, *Small* **2012**, 8, 3584. c) J. Liu, Z.K. Sun, Y.H. Deng, Y. Zou, C.Y. Li, X.H. Guo, L.Q. Xiong, Y. Gao, F.Y. Li, D.Y. Zhao, *Angew. Chem.* **2009**, 121, 5989.

9 a) B.J. Li, H.Q. Cao, J. Shao, M.Z. Qu, *Chem. Commun.* **2011**, 47, 10374. b) M. Zhang, M.Q. Jia, *J. Alloys and Compounds* **2013**, 551, 53. c) Y. Chen, B.H. Song, X.S. Tang, L. Lu, J.M. Xue, *J. Mater. Chem.* **2012**, 22, 17656.

10 F. Zhang, T.F. Zhang, X. Yang, L. Zhang, K. Leng, Y. Huang, Y.S. Chen, *Energy. Environ. Sci.* **2013**, 6, 1623.

11 Y.C. Dong, R.G. Ma, M.J. Hu, H. Cheng, C.K. Tsang, Q.D. Yang, Y.Y. Li, J.A. Zapien, *J. Solid State Chemistry* **2013**, 201, 330.

12 a) D.W. Su, H.S. Kim, W.S. Kim, G.X. Wang, *Microporous and Mesoporous Materials* **2012**, 149, 152. b) J. Chen, L. Xu, W. Li, X. Gou, *Adv. Mater.* **2005**, 17, 582.

13 a) Z.C. Yang, J.G. Shen, L.A. Archer, *J. Mater. Chem.* **2011**, 21, 11092. b) Y.Z. Piao, H.S. Kim, Y.E. Sung, T. Hyeon, *Chem. Commun.* **2010**, 46, 118. c) S. Grugeon, S. Laruelle, L. Dupont, J.M. Tarascon, *Solid Stae Sci.* **2003**, 5, 895.

14 S. Laruelle, S. Grugeon, P. Poizot, M. Dolle, L. Dupont, J.M. Tarascon, *J. Electrochem. Soc*. **2002**, 149, A627.